American Mineralogist, Volume 59, 190–200, 1974

Selected Area Electron Diffraction Study of a Type II "Valleriite-Like" Mineral

N. I. ORGANOVA

Institute of the Geology of Ore Deposits, Petrography, Mineralogy, and Geochemistry of the USSR Academy of Sciences, Moscow, USSR

V. A. DRITS, AND A. L. DMITRIK

Institute of Geology of the USSR Academy of Sciences, Moscow, USSR

Abstract

Selected Area Electron Diffraction studies of the "valleriite-like" mineral type II of Harris and Vaughan (1972) show it to be a mixture of tochilinite, 6 $Fe_{0.9}S \cdot 5[(Mg,Fe)(OH)_2]$, and two new hybrid structures, designated Phase 1 and Phase 2. Phase 1 is formed of alternating layers of sulfide, $Fe_{0.78}S$, and brucite $(Mg,Fe)(OH)_2$. The sulfide layers have a mackinawite-type structure with a regular chessboard arrangement of vacancies. The relative displacement of the neighboring sulfide layers resembles that of tochilinite and gives rise to a one-layer unit cell, space group $P1$, $a = b = 3.68$ Å, $c = 10.92$ Å, $\alpha = \beta = 93.5°$, $\gamma = 90°$. The neighboring brucite component consists of two single brucite layers, one rotated 22° to the other to form a sublattice with a two-layer unit cell, space group $P1$, $a = 8.31$ Å, $b = 14.4$ Å, $c = 21.84$ Å, $\alpha = \beta = 93.5°$, $\gamma = 90°$. The chemical formula is 2 $Fe_{0.98}S \cdot 1.58[(Mg,Fe)(OH)_2]$.

In Phase 2, sulfide layers having the same crystallo-chemical characteristics as those of Phase 1 alternate with layers whose dimensions in the (001) plane are $a = 8.18$ Å, $b = 3.68$ Å, $\gamma = 90°$. The following model is suggested for these latter layers: within a layer, octahedra consisting of hydroxyls and water molecules with Fe cations at their centers share edges to form chains parallel to the b-axis. Linked by their free apices, these chains of octahedra form flat networks with water molecules in the "windows." The chemical formula for this structure is 20 $Fe_{0.78}S \cdot 9$ $[Fe(OH)_2\ 3/2\ H_2O)]$.

These two new phases should be classified, along with tochilinite-I and tochilinite-II, into the tochilinite mineral group, which differs from the valleriite group in the structure of the sulfide layer.

Introduction

Evans and Allmann (1968), in a paper on the structure determination of valleriite, first demonstrated the possibility of minerals formed of alternating sulfide and brucite layers. In valleriite, the sulfide layers of composition $Fe_{1.07}Cu_{0.93}S_2$ alternate along the c axis with brucite layers of composition $Mg_{0.68}Al_{0.32}(OH)_2$. Thus, the ore and non-ore components are coherently interstratified within one crystal. The sulfide layer of valleriite can be described as a set of sulfur tetrahedra, statistically populated by Fe and Cu atoms, with their bases parallel to the (001) plane and their apices turned alternately upwards and downwards. Each tetrahedron shares three lateral edges with the adjacent tetrahedra (Fig. 1). The fact that anions of different kinds are packed compactly within each layer results in the incommensurability of the unit cells of the sulfide and non-sulfide layers (Fig. 2). Thus the mineral must be described by two sets of crystallographic parameters. In the sulfide component of valleriite, these are: space group $R\bar{3}m$, $a = 3.79$ Å, $c = 34.10$ Å, and for the brucite component, $P\bar{3}m$, $a = 3.07$ Å, $c = 11.37$ Å.

Two similar "fibrous Fe-sulfide" finds have been described from Muskox, Canada (Jambor, 1969) and from Cornwall, England (Clark, 1970). In both cases, however, detailed study was hampered by small grain size. Electron probe analyses showed the contents as Fe, Mg, and S.

A mineral from the Mamonovo deposit, Voronezh Region, USSR, belongs to the same group. Thorough chemical and diffraction analyses of the material found in inclusions proved that it belonged to a new mineral species, which was named tochilinite (Or-

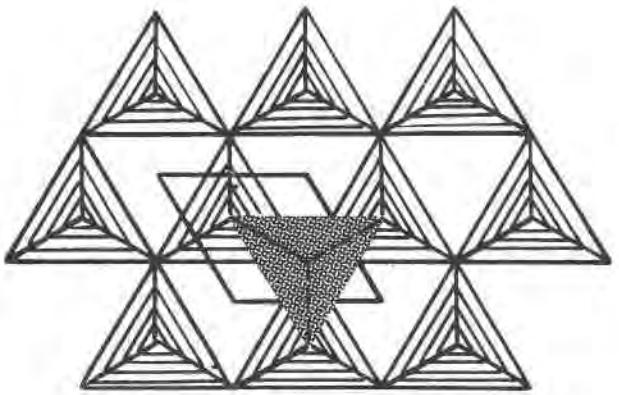

FIG. 1. Projection normal to (001) of the sulfide tetrahedra in valleriite. For greater clarity, tetrahedra with upward apices are presented, but only one (shaded) tetrahedron of those with a downward apex. The unit cell is shown.

ganova *et al,* 1971; Organova, Drits, and Dmitrik, 1972). Tochilinite, 6 $Fe_{1-x}S \cdot 5[(Mg,Fe)\ (OH)_2]$, occurs in two morphological varieties, granular and acicular (neither of which forms a macrocrystal). Structurally it consists of alternating sulfide and brucite layers. The sulfide layers resemble those of mackinawite, a tetragonal layer mineral of formula FeS (Berner, 1962) and with $a = 3.68$ Å. Figure 3 shows the projection normal to (001) of the sulfide layer in mackinawite, a set of tetrahedra lying on their lateral edges, each tetrahedron sharing four edges with its neighbors.

In tochilinite, the sulfide layers contain vacancies distributed in a regular pattern; Figure 4 shows the normal idealized projection of the sulfide layer in granular tochilinite (tochilinite-I). The acicular variety of tochilinite consists of two crystal phases,

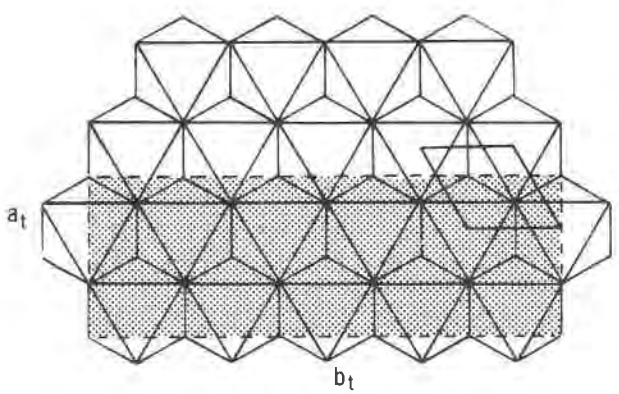

FIG. 2. Projection normal to (001) of the octahedra in the brucite layer of valleriite. The solid line shows the unit cell of valleriite; the shaded rectangle that of tochilinite.

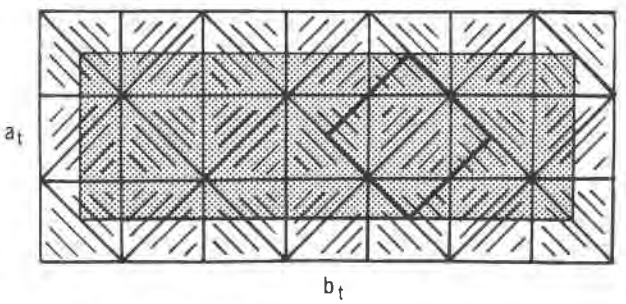

FIG. 3. Projection of normal to (001) of the sulfide tetrahedra in mackinawite. Unit cells of mackinawite (thick line) and tochilinite (shaded rectangle) are shown.

tochilinite-I (analogous to the granular variety) and tochilinite-II, which differs from tochilinite-I in the distribution of the vacancies in the sulfide layer (Fig. 5) (Organova, Drits, and Dmitrik, 1973a). In both tochilinites the neighboring sulfide layers are shifted in relation to one another by $-1/6a$.

In tochilinite-I the sulfide and brucite layers have the same unit cell (Figs. 2, 4). For space group $C1$, these layers have $a = 5.37$ Å, $b = 15.60$ Å, $c = 10.72$ Å, $\alpha = \gamma = 90°$, $\beta = 95°$, $3\ a \simeq b$. In tochilinite-II the two layers have differing unit cells; the brucite layer is nearly identical with that for tochilinite-I, while for space group $P1$ the sulfide layer has $a = 8.34$ Å, $b = 8.54$ Å, $c = 10.74$ Å, $\alpha = 87.3°$, $\beta = 94.5°$, $\gamma = 92°$. However, the coincidence of reflections of a common type from both components of tochilinite-II makes it possible to describe both sub-lattices in terms of a single larger unit cell.

Dr. Harris kindly sent us a polished section of the material from Pephkos, Cyprus, a "valleriite-like" mineral, type II, studied by Harris and Vaughan (1972), which we find to have an X-ray powder

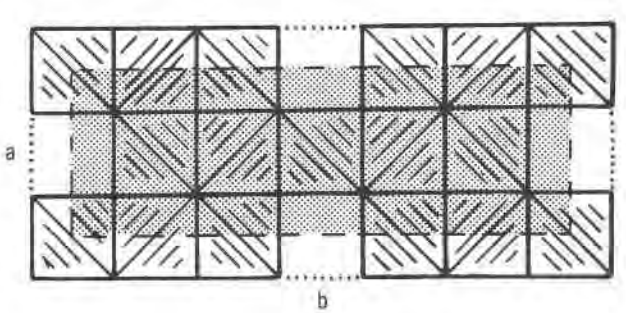

FIG. 4. Idealized projection normal to (001) of the sulfide tetrahedra in tochilinite-I. Tetrahedra incompletely populated by iron atoms are not drawn and thus appear as blank squares, one side of which is dotted. The unit cell of tochilinite is lightly shaded.

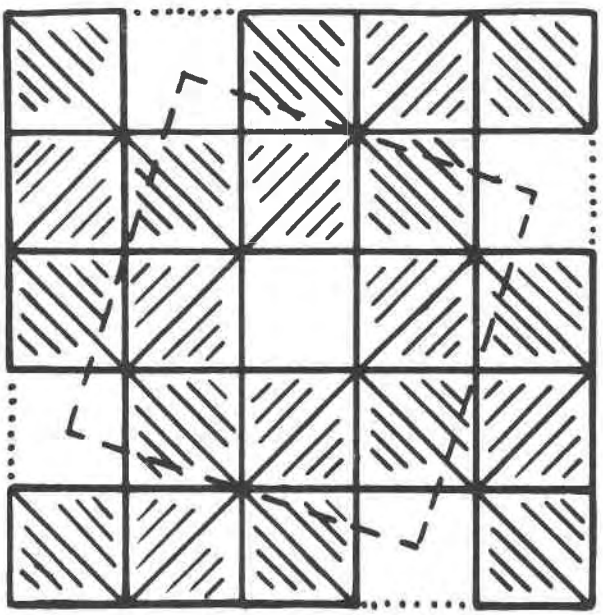

FIG. 5. Idealized projection normal to (001) of the sulfide tetrahedra of tochilinite-II. The dashed outlines represent the unit cell of the sulfide component of the structure.

pattern and composition close to tochilinite. Within this same material Harris and Vaughan also identified a "valleriite-like" mineral, type I.

Method of Structural Investigation

The fact that hybrid minerals with a sulfide component occur only in finely dispersed inclusions and often in minor quantities is explained by their structural features and apparent conditions of formation. This is precisely the reason why the valleriite structure remained undetermined for so long. Only after discovering a monocrystal in the African deposit at Loolecop were Evans and Allmann (1968) able to establish that the mineral discovered a hundred years before was not merely a sulfide of copper and iron. Even for tochilinite, which was found not only in a dispersed form but with an acicular texture, the structural model could be proposed and reliably confirmed only with the aid of the Selected Area Diffraction method (SAD).

SAD patterns from micromonocrystals afford, under favorable conditions, the opportunity to obtain rational sections of the reciprocal lattice and thus to obtain information about the projection of the structure in the direction coinciding with the electron beam (Vainshtein, 1964; Zvyagin, 1967). The layer structure and resulting basal cleavage of the minerals belonging to the valleriite and tochilinite groups facilitated the choice of micromonocrystals with the appropriate orientation for the electron beam. SAD pattern intensities have not been widely applied thus far in structural studies because of a number of difficulties inherent to the process. The major difficulties notably related to extinction effects are (1) it is not always easy to take account of the nature of interaction between the electrons and the crystal (whether kinematic or dynamic), especially for crystals of an unknown structure; (2) one does not always know in advance what additional factors, depending on the mosaicity of the specimen, should be introduced for conversion of intensities to structural amplitudes; (3) the scattering from different volume elements can contribute to different reflections. However, the determination of the tochilinite structure has proved that these difficulties can be surmounted to obtain sufficiently reliable structural models.

The intensities on the photographic plates were measured visually using multiple exposures for strong reflections and calibrated blackening marks for weak ones.

The use of X-ray powder patterns alone for diagnosis of sulfide-component hybrid structures can lead to an error. In particular, a tochilinite X-ray powder pattern may be indexed in terms of the valleriite unit cell. On the other hand, even a visual observation of electron diffraction patterns permits a reliable distinction between valleriite and tochilinite (see SAD patterns for valleriite and tochilinite, Figures 6 and 7). Whereas Figure 6 shows two systems of double maxima with hexagonal symmetry, the reflections from the tochilinite monocrystal form an orthorhombic motif, characteristic of this mineral (Fig. 7). The present investigation also shows that this method can clearly distinguish between different representatives of the tochilinite group. For example, electron diffraction patterns for the valleriite-like mineral of type II included not only patterns typical of other hybrid structures with a sulfide component but also patterns not previously observed which convey the material's distinctiveness.

The thin section placed at our disposal (Harris and Vaughan, 1972) contained, in the troilite mass, not only minor inclusions of the "valleriite-like" mineral of type-II, but also, rimming these inclusions, the type-I "valleriite-like" mineral. Both types of the "valleriite-like" mineral are in close spatial contact and may be admixed; therefore, a diffraction study

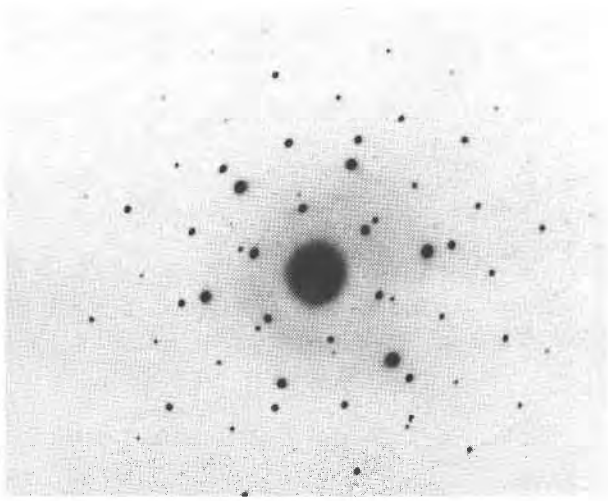

FIG. 6. Selected area pattern of valleriite.

would be incomplete without investigation of the type-I mineral by electron microscope. Nevertheless, we failed to decipher the type-I structure, nor are we able to propose for it even a hypothetical model.

The bulk of the material gives a diffraction pattern with hexagonal symmetry. Cell dimensions in the plane of the sample are smaller than the rhombohedral unit cell of calcite; these measurements were corroborated by the SAD pattern for calcite. In the (0001) plane using hexagonal axes, a equals 4.99 Å for calcite and 4.32 Å for "valleriite-like" mineral type-I.

The thin section provided by Dr. Harris contained two noticeable type-II inclusions, but its small volume did not allow any final conclusion on the quantitative relationships of its components. Material taken from different places on the thin section showed differing frequencies of diffraction, but the shortage of material precluded controlled testing of these differences in X-ray powder patterns.

First area of the thin section

The bulk of the material is tochilinite analogous to the granular (tochilinite-I) variety. The microcrystals are elongated along the b axis (Fig. 7), as in granular tochilinite (Organova, Drits, and Dmitrik, 1972). SAD patterns gave $a \sin \beta = 5.28$ Å, $b = 15.7$ Å. If we assume that $\beta = 95°$ as in the tochilinites, then $a = 5.32$ Å, i.e. $3a \simeq b$.

Like the tochilinites and valleriites, hexagonal and pseudohexagonal arrangements of reflections occur among the diffraction patterns, (*e.g.* Fig. 8). Most probably they are associated with $Fe(OH)_3$, the SAD patterns of valleriite type II being similar to those of tochilinite in which $Al(OH)_3$ was proved (Organova, Drits, and Dmitrik, 1972).

Figure 9 presents the SAD pattern corresponding to the essentially new structure that we have named Phase 1. The strongest reflections form a square network corresponding to $a = 3.68$ Å, as in mackinawite (Berner, 1962). Thus the square system of reflections stems from the sulfide part of the structure. The connection between the coordinate axes of tochilinite and the sulfide part of Phase 1 can be expressed by vector relationships (Fig. 3):

$$\vec{A}_1 = 1/6\ \vec{b}_{\text{toch}} + 1/2\ \vec{a}_{\text{toch}}$$
$$\vec{B}_1 = -1/6\ \vec{b}_{\text{toch}} + 1/2\ \vec{a}_{\text{toch}}$$

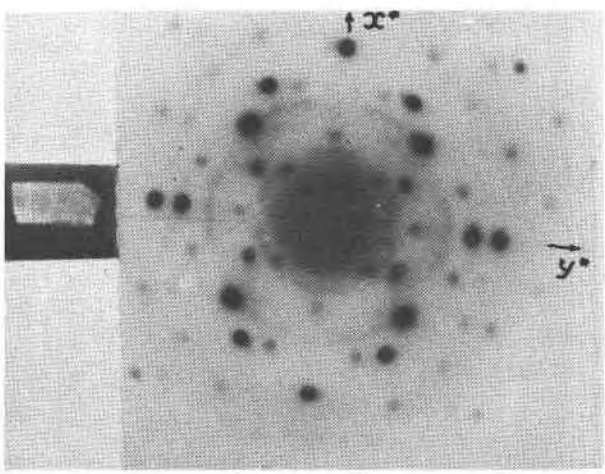

FIG. 7. Selected area pattern of tochilinite obtained from the "valleriite-like" mineral, type-II.

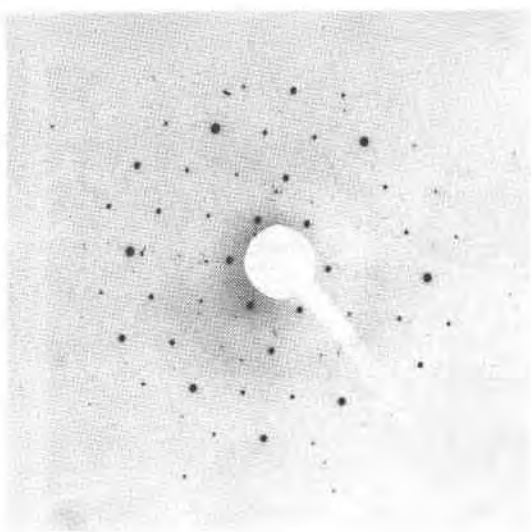

FIG. 8. Selected area pattern with pseudo-hexagonal symmetry [$Fe(OH)_3$].

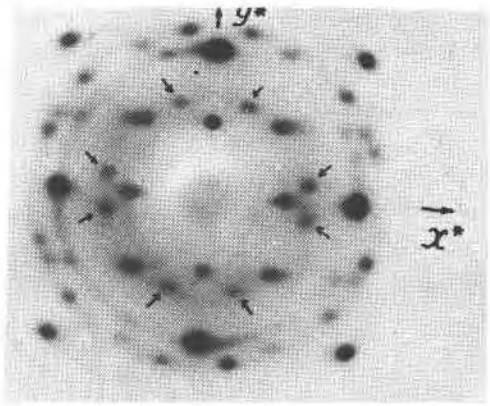

FIG. 9. Selected area diffraction pattern of Phase 1.

The less intense set of reflections separate from the sulfide ones can be naturally associated with diffraction from the brucite component. The two pairs which are adjacent to the sulfide reflections 100 and 010 (indicated by arrows, Fig. 9) are at equal distances from the incident electron beam, and have $d = 2.72$ Å (identified with 100 of brucite in hexagonal axes). This corresponds to $a = 3.14$ Å. Some of the angles between the reflections = 60°.

The next system of reflections equidistant from the incident beam lies at a distance greater by $\sqrt{3}$ from the first system. Figure 10 gives the scheme of arrangement of all reflections of Figure 9, but the SAD pattern contains a number of reflections that do not fit into this scheme.

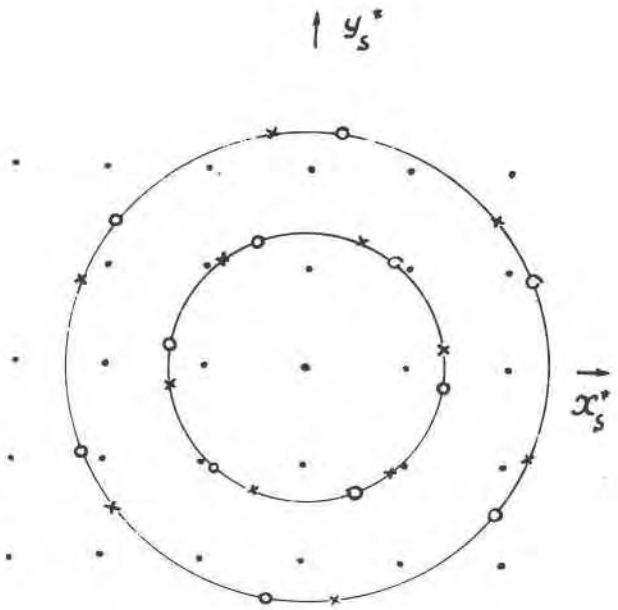

FIG. 10. Scheme of selected area electron diffraction pattern of Phase 1. The dots represent sulfide reflections. The open circles and crosses represent the two systems of brucite reflections.

Second area of the thin section

Figure 11 shows the most frequent type of diffraction pattern, other than the tochilinite one. The most intense reflections form a square network similar to the sulfide reflections of Phase 1; these are accompanied by additional reflections, as indicated by arrows in Figure 11. If the square system corresponds to $a_{sq} = 3.68$ Å, then for the second system with orthorhombic geometry and the same distribution of intensities, $a = 4.09$ Å, $b = 3.68$ Å, where $9a = 10a_{sq}$. Subsequent investigation has shown that the real size of a is $4.09 \times 2 = 8.18$ Å.

Structure of Phase I

For a detailed identification of the structure of the sulfide layer, the intensities of the 12 independent reflections on the pattern given on Figure 9 were measured. The formula $\phi \sim \sqrt{I/d}$, which according to Vainshtein (1964) is correct for cases in which considerable angular variation of mosaic blocks (3–4°) makes up the crystal, was used to convert intensities to structural amplitudes. Patterson projections (Fig. 12) have maxima conforming to the mackinawite model. Thus at $u = 0.5$, $v = 0$ and at $u = 0$, $v = 0.5$ the ends of vectors Fe–S are found, and at $u = 0.5$, $v = 0.5$, those of Fe–Fe and S–S. However, the "weight" of the former two peaks is greater than that of the latter peak; therefore, the position corresponding to the Fe atom in the center of the unit cell is not completely filled. Estimation

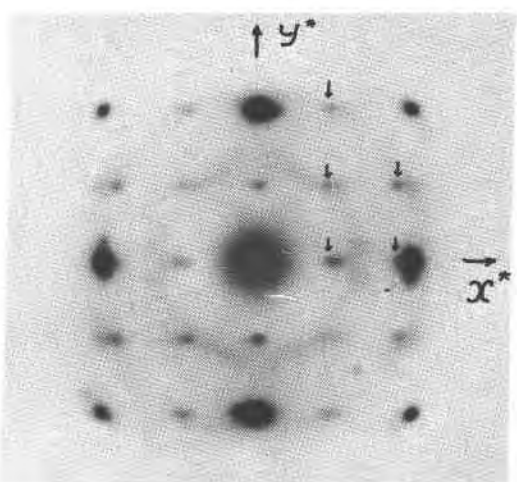

FIG. 11. Selected area pattern of Phase 2.

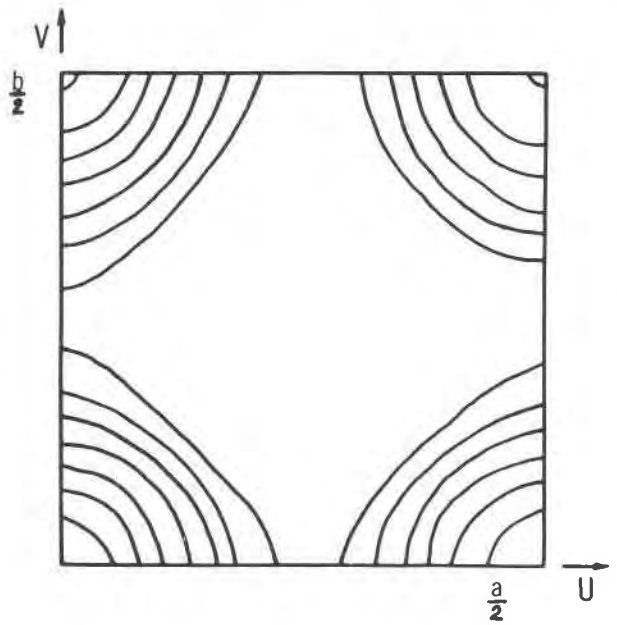

FIG. 12. Patterson projection of the sulfide component of Phase 1 along the *c* axis.

of the relative height of the Patterson peak at $u = 0.5$, $v = 0.5$ showed that the content of this Fe site is 0.5 instead of unity as required by space group *4mm* for that point. Identification of all atoms, taking into account the incomplete filling of one of the Fe atom sites, gave $R = 15$ percent. Using the least squares method to determine the general thermal constant and the content of the Fe atom site at $x = 0.5$, $y = 0.5$, the value of the residual factor was refined to $R = 13.9$ percent for 0.55 occupancy and $B = 5$. Table 1 gives the experimental and theoretical values of the structural amplitudes of the sulfide component of Phase 1. Figure 13 shows the structure of the sulfide layer in polyhedra projected along *c*. Tetrahedra with vacancies having a chessboard arrangement are shown empty. A unit cell contains (1 + 0.55) Fe atoms for every 2 S atoms. Thus the formula becomes $Fe_{1.55}S_2 = 2\ Fe_{0.78}S$.

Additional data on the brucite component of Phase 1 may be obtained by comparing the scheme of Figure 10 with the SAD pattern (Fig. 9). Apart from reflections indicated on the scheme, the plate has additional reflections. These suggest a brucite sub-lattice whose unit cell contains two brucite layers, one rotated relative to the other. This large unit cell (1) explains the appearance of all reflections (which would be absent in a simple noncoherent superposition of two one-layer brucite sub-lattices turned relative to each other); and (2) perturbs the

TABLE 1. Experimental and Calculated Structural Amplitudes of the Sulfide Component of Phase 1

hkl	$\lvert\phi_{ex}\rvert$	ϕ_{calc}	*hkl*	$\lvert\phi_{ex}\rvert$	ϕ_{calc}
010	1.8	1.94	310	0.410	0.148
020	5.92	6.01	410	0.27	0.119
030	0.33	0.36	220	2.31	2.79
040	0.89	0.85	320	0.254	0.201
110	0.69	-0.165	420	0.4	0.499
210	0.432	0.70	330	0.28	0.082
			B = 5		R = 13.9%

strict hexagonality of intensity distributions for each of the two "brucite" systems of reflections presented on Figure 10. It should be noted that neither the deviation from hexagonality nor the intensities of the additional reflections is great.

All "brucite" reflections of Figure 9 fit in the unit cell whose coordinate axes coincide in direction with the *a* and *b* axes of the sulfide sub-lattice and are $A_{br} = 8.31$ Å, $B_{br} = 14.4$ Å, $\gamma = 90°$.

To determine the rotation angles of the neighboring brucite layers and the relative rotation angles of the sulfide and brucite components, various alternatives were considered. These were obtained in the following way. Two identical sets of unit cells of the brucite layer were drawn in the form of rhombuses on two pieces of tracing paper at an arbitrary scale (Fig. 14). The tracing papers were then superimposed so that two apices of the unit cells coincided. Rotating the upper tracing paper in relation to the lower one, three different and independent variants were found

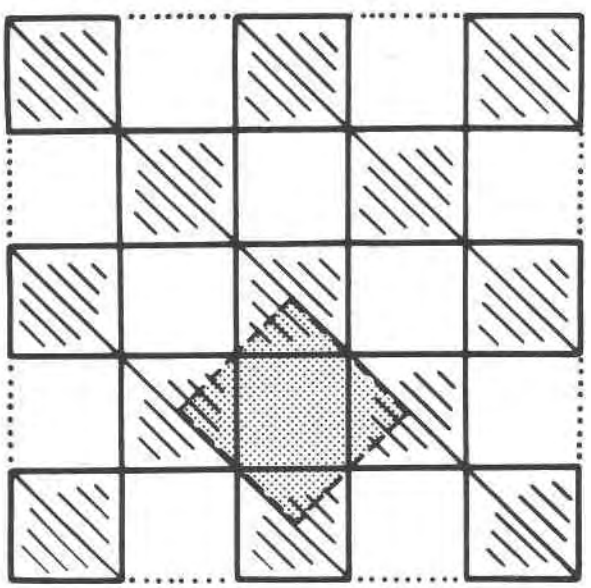

FIG. 13. Projection of the sulfide layer of Phase 1 in polyhedra. Tetrahedra incompletely occupied by iron atoms are shown empty. The unit cell is shaded.

that corresponded geometrically to experiment. An admissible variant was assumed to be that for which a large unit cell with perpendicular axes, common for the two systems and having the above dimensions, was formed. The variants thus found were used for calculation of the theoretical intensities. The best coincidence with the experiment was shown by the variant presented on Figure 14. On Figure 15, the results of the calculation of theoretical intensities for the optimum variant are indicated by circles in the scale of the reciprocal space, the size of the circle being proportional to the intensity value. The common design of the strongest intensities corresponds to the "brucite" reflections present on Figure 9. Figure 14 shows that the dimensions of the unit brucite rhombus are connected with the parameters of the large "brucite" unit cell of Phase 1 by relations: $A_{com} = a_{br}\sqrt{7} = 8.31$ Å, $B_{com} = a_{br}\sqrt{21} = 14.4$ Å. The relative rotation of the neighboring brucite networks is 22°. The rotation of each of them in relation to the "sulfide" axes is computed to be 41° for one and approximately 19° for the other. These values of the angles agree with the measurements on the selected area electron pattern of Figure 9. In effect, the angle between the vertical pair of "brucite" reflections is 22°, and the relationships between the other angles can be found in a similar way.

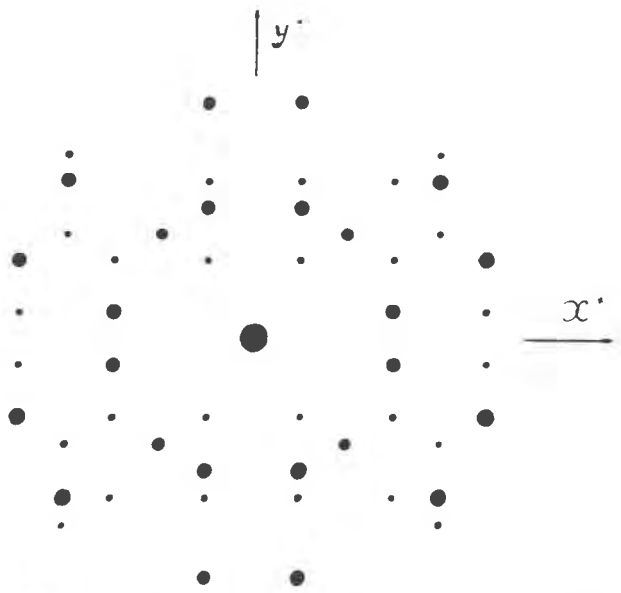

FIG. 15. Theoretical intensities of the brucite component of Phase 1, plotted in reciprocal space.

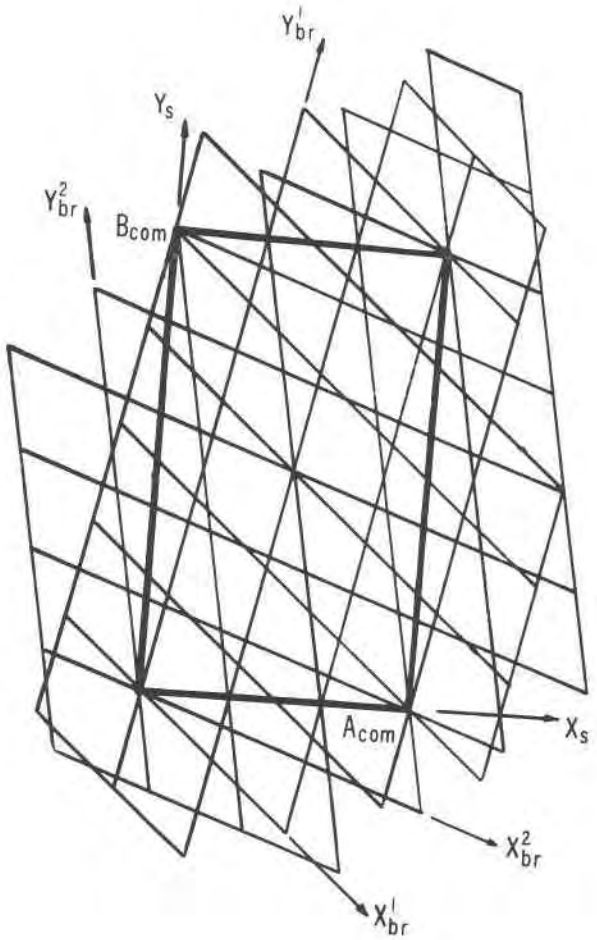

FIG. 14. Relative arrangement of the neighboring brucite networks in Phase 1. Small rhombuses designate the unit cell of the initial brucite network. Thick line shows the common resultant unit cell of the brucite component of Phase 1. The x and y axes for the two brucite layers are differentiated by the superscripts 1 and 2. The axes for the resultant unit cell are labelled x_s and y_s.

The measured intensities of the sulfide and brucite sub-lattices agree with the theoretical values of intensities.

The factor for the brucite molecule in the formula of Phase 1, as well as for other hybrid structures, is equal to the ratio of the area per one sulfur atom to the area per one hydroxyl in the plane (001). In this case, it is the ratio of the area of the unit sulfide square—$3.68^2 = 13.5$ Å^2—to the area of the small brucite rhombus,

$$\frac{a^2_{br}\sqrt{3}}{2} = \frac{3.14^2\sqrt{3}}{2} = 8.60 \text{ Å}^2,$$

and is equal to 1.57.

The relative positions of the sulfide layers of the structure cannot be determined by SAD. However,

the presence on the X-ray powder pattern of only the lines indicated in the tochilinite unit cell (Table 2, column II) and the absence of additional reflections can serve as a proof (given a sufficient amount of Phase 1 to produce an X-ray powder pattern) of the fact that the relative displacement of the sulfide layers of the sample is analogous to that in tochilinite. This means that every next layer is displaced in relation to the preceding one by $-1/6$ of the diagonal of the unit square. Then for the sulfide sublattice we have: $a = b = 3.68$ Å, $c = 10.92$ Å, $\alpha = \beta = 93.5°$, $\gamma = 90°$.

Table 2 presents the X-ray powder data obtained by Harris and Vaughan (1972) for the valleriite-like mineral (Type II). Column II of this table gives the *hkl*'s on the basis of a tochilinite unit cell, and column III those for the sulfide subcell defined above. The connection between the indices of columns 2 and 3 is readily found by the vector relationship between the coordinate axes:

$$H = \frac{6h_{toch} + k_{toch}}{6}, \qquad K = \frac{6h_{toch} - k_{toch}}{6}$$

Therefore, the powder X-ray pattern data do not disagree with the hypothesized displacement of the sulfide layers.

Hence, Phase 1 is a hybrid structure, in which mackinawite-like layers with their peculiar distribution of vacancies alternate along the c axis with brucite layers. Brucite layers are turned in relation to the sulfide ones, and apparently form a two-layer unit cell. The formula of Phase 1 can be written as 2 $Fe_{0.78}S \cdot 1.57$ $[(Mg,Fe)(OH)_2]$. The negative charge of the sulfide layer can be compensated if part of iron in the brucite layer is in the trivalent state.

TABLE 2. X-Ray Powder Pattern of "Valleriite-Like" Mineral (Type II)

N	I*	d_{meas}*	I* hkl	II** hkl	III*** hkl	d_{calc}
1	8	10.86	003	001	001	
2	10	5.42	006	002	002	
3	2	3.606	009	003,13$\bar{1}$	003,10$\bar{1}$	3.58
4	0.5	3.222	101	--	--	
5	3	2.713	00.12.	004,13$\bar{3}$	004,10$\bar{3}$	2.72
6	4	2.602	--	060,151	1$\bar{1}$0	2.61
7	0.5	2.535	108	061,133	11$\bar{1}$,10$\bar{3}$	2.53,2.55
8	4	2.301	10.10	202,062	112,1$\bar{1}$2	2.27,2.34
9	3	2.233	--	20$\bar{3}$,13$\bar{4}$	11$\bar{3}$,10$\bar{4}$	2.21,2.25
10	2	2.183	00.15	005	005	
11	2	2.125	--	063,134	1$\bar{1}$3,104	2.11,2.12
12	0.5	1.876	110	064,204	11$\bar{4}$	1.879
13	5	1.838	113	26$\bar{1}$,13$\bar{5}$	201,10$\bar{5}$	1.835,1.832
14	3	1.804	00.18	006,26$\bar{1}$	20$\bar{1}$	1.813
15	2	1.571	00.21	007,13$\bar{6}$	10$\bar{6}$	1.585
16	2	1.351	00.24	008,067	11$\bar{7}$	1.359

*I After Harris and Vaughan, 1972, a = 3.74Å, c = 32.64Å.
**II For tochilinite; a = 5.32Å, b = 15.7Å, c = 10.92Å, $\alpha = \gamma = 90°$, $\beta = 95°$.
***III For phase 1. a = b = 3.68Å, c = 10.92Å, $\alpha = \beta = 93.5°$, $\gamma = 90°$.

Structural Model for Phase 2

The similarity of the square motifs on diffraction patterns of Phase 1 and Phase 2 suggests that their sulfide components are structurally identical. It thus appeared natural to associate the additional reflections with the hydroxide sublattice.

The peculiar feature of the SAD patterns for Phase 2 is the modification of the intensity distribution usual for "brucite" reflections. The intensities of the non-sulfide part of the diffraction picture were measured from several different SAD patterns of Phase 2. As the diffraction pictures from different sub-lattices coincided for reflections $0k0$, the approximate contribution from the non-sulfide component was estimated as the difference of intensities $0k0$ and $h00$ of the sulfide component. For the conversion from intensities to structural amplitudes the formula $\phi \sim \sqrt{I/d}$ was used. One of the Patterson syntheses obtained (Fig. 16) corresponds to the selected area diffraction pattern (Fig. 11). Despite smearing of

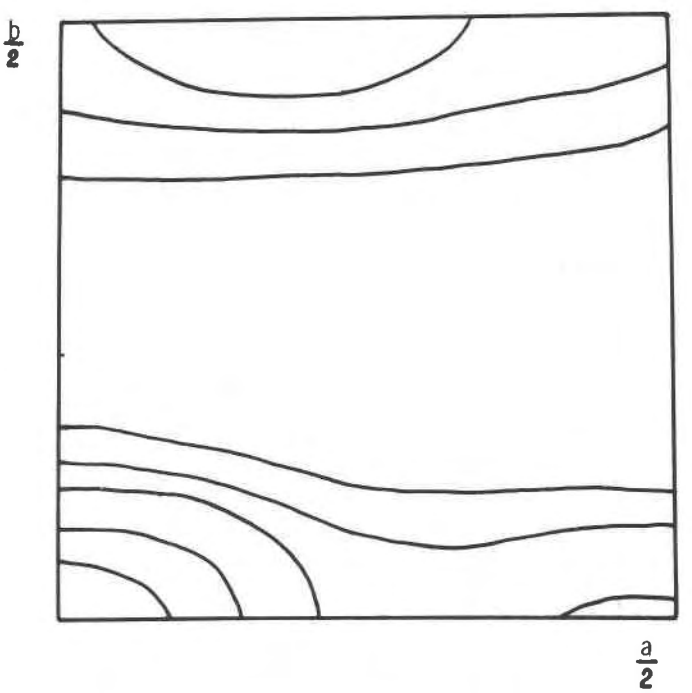

FIG. 16. Patterson synthesis of the non-sulfide component of Phase 2.

the Patterson function, two maxima can be distinguished: one for $u = 0.16$, $v = 0.5$, the other for $u = 0.5$, $v = 0$. It should be noted that on Patterson maps constructed on the basis of intensities from other crystals, the Patterson function retains its general character, although the position of the strongest maximum at $v = 0.5$ is changed. The value of u in that case decreases to 0.1.

Attempts at interpreting the maxima on the Patterson snythesis on the hypothesis of a brucite-like layer failed. Indeed, the arrangement of atoms of a brucite layer which is hexagonal in projection would appear not only on the Patterson synthesis but also in the arrangement of reflections on the selected area pattern. Assuming that the two maxima of roughly the same height on the Patterson synthesis correspond to two oxygens, each linked to the metal atom at the origin of coordinates, one can arrive at the model presented in Figure 17.

The octahedra composed of OH groups and molecules of H_2O have Fe atoms at their centers. By their common lateral edges they are linked into chains aligned along b. The neighboring chains are linked by free apices to form a two-dimensional network. Water molecules are located at the common apices of octahedra, and the common edges are formed by the hydroxyls. In addition water molecules designated by circles (Fig. 17) are located in the empty "windows" of the structure (introduction of these molecules improved the agreement with experimental data). An indirect confirmation of the presence of water weakly associated with the structure seems to be given by the fact that bubbles were formed on the micromonocrystals of Phase 2 in the electron microscope. Bubbles were not observed for micromonocrystals having other types of diffraction motifs. The best agreement with the experimental data was shown by the model in which a half water molecule occurs on average in every "cavity." Because of this peculiarity of the structure, the quantity of water sometimes decreases during observation in the electron microscope, which may be a reason for a change in the distribution of reflection intensities. Migration of a part of water from the structure must lead to a shifting of OH groups; this is in fact shown by the shifting of the peak on the Patterson map for different monocrystals. Table 3 gives experimental and calculated structural amplitudes for the hydroxide component of Phase 2, and Table 4 gives coordinates of the atoms. The R-factor, 25.2 percent, shows that the model may be regarded as possible but is not proved unambiguously. The same conclusion is suggested by the evaluation of the possible interatomic distances. This was done on an assumption that the thickness of the unit layer of Phase 2 is the same as that of the other two crystal phases present in the sample. The Fe–OH distance is then 2.19 Å, a value at the upper limit admissible for divalent iron. However, the presence of vacancies in the sulfide layer of Phase 2 should, by analogy with other hybrid structures, lead to a negative charge and hence to a surplus positive charge in the non-sulfide layer. Then a part of iron in the hydroxide layer must be trivalent, which does not conform to the interatomic distance Fe–OH.

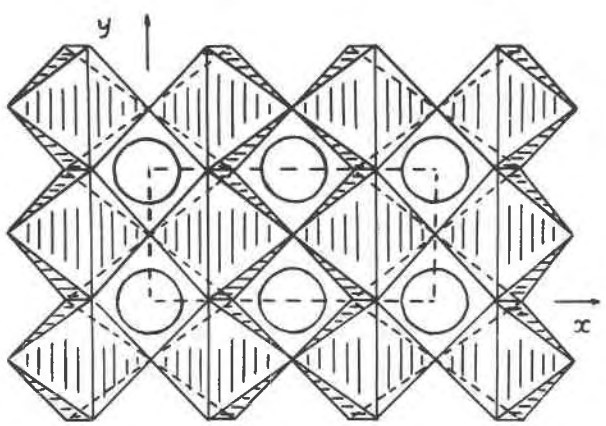

FIG. 17. Projection along c with the hydroxide component of Phase 2.

The chemical formula of Phase 2 can be obtained by comparing the composition for the general large unit cell for different components. The dimensions of the unit cell in the layer plane for the sulfide and hydroxide sub-lattices coincide along b, while along a they relate as 10 to 9. Then, as the unit cell of the sulfide component of the mineral accounts for 2 $Fe_{0.78}S$, and the unit cell of the hydroxide component accounts for $Fe(OH)_2 \cdot 3/2\ H_2O$, the formula can be written as 20 $Fe_{0.78}S \cdot 9\ [Fe(OH)_2 \cdot 3/2\ H_2O]$. The factor 3/2 before H_2O is due to the fact that, per unit cell, there is one water molecule at $x = 0.5$, $y = 0.17$ and 1/2 H_2O at $x = 0.5$, $y = 0.5$ (see Fig. 17).

The comparison of the chemical formulas of Phase 1 and Phase 2 shows that the number of atoms functioning as anions in the non-sulfide parts of the structures is practically the same. Notably, in Phase 1 for 2 $Fe_{0.78}S$, there are $1.57 \times 2 = 3.24$ hydroxyl groups while in Phase 2, taking OH and H_2O together there are $(2 + 3/2) \times 0.9 = 3.15$. However,

the number of non-sulfide cations in Phase 2 per 2 $Fe_{0.78}S$, 0.9 Fe, is smaller than in Phase 1, 1.57 (Mg,Fe).

Summary

According to the results of the SAD analysis, the sample from Harris and Vaughan contains:

1. Tochilinite proper, having the formula 6 $Fe_{0.9}S \cdot 5$ $[(Mg,Fe)(OH)_2]$, which can be re-written as 2 $Fe_{0.9}S \cdot 1.67$ $[(Mg,Fe)(OH)_2]$
2. Phase 1, with the formula 2 $Fe_{0.78}S \cdot 1.57$ $[(Mg,Fe)(OH)_2]$
3. Phase 2 with the formula 2 $Fe_{0.78}S \cdot 0.9$ $[(Fe(OH)_2 3/2\ H_2O]$
4. Pseudohexagonal Fe $(OH)_3$

In calculating the formula 2 $FeS \cdot 1.58$ $[Mg_{0.53}Fe_{0.47}(OH)_2]$ from their electron probe analysis, Harris and Vaughan (1972) assumed a valleriite-like sulfide layer with a 1:1 cation-anion ratio. They note that: (1) the sum of the weight percentages determined is 79.2 percent; (2) the calculated OH content is 22.03 percent; and (3) the grand total of both is 101.2 percent. Although realizing that all methods for calculating structural formulas for mixtures of minerals are approximate at best, we have recalculated their data under the assumption of a cation deficiency in the sulfide layer (as proved for tochilinite). This re-calculation, which leads to the formula 2 $Fe_{0.88}S \cdot 1.82$ $[Fe_{0.54}Mg_{0.46}(OH)_2]$, also assumed that the grand total was 100 rather than 101.2 percent (the calculated OH content is 20.8 percent). The factor of 1.82 for the brucite molecule, a value in excess of the theoretical 1.67, we attributed to the presence of $Fe(OH)_3$. It should be mentioned that for tochilinite (Organova *et al,* 1971) conformity to the theoretical value was obtained only after all Al was consigned to $Al(OH)_3$. The structural formula calculated by Harris and Vaughan (1972) for granular tochilinite differs from ours (Organova *et al,* 1971) and from the theoretical formula mostly because of the admixtures of the $Al(OH)_3$ type.

On the Crystal Chemistry of Hybrid Structures with a Sulfide Component

The names, chemical formulas, and crystallochemical characteristics of known hybrid structures with a sulfide component are tabulated in Table 5.

Incommensurability of the ionic radii of sulfur and hydroxyl in the case of identical packing of anions in the sulfide and brucite layers of valleriite gives rise to differing sub-lattices. The same reasoning explains the appearance of a non-stoichiometric factor in the chemical formula of the mineral. The layers are held together by electrostatic forces (as is evidenced by the presence of trivalent aluminum in the brucite layer). The relative displacement of the neighboring sulfide layers in a majority of valleriites takes place at 1/3 of the long diagonal of the unit rhombus (Fig. 1); this gives rise to a three-layer rhombohedral cell. A one-layer modification of the mineral has also been found (Organova, Drits, and Dmitrik, 1973b) in which no shifting of the neighboring sulfide layers is observed.

TABLE 3. Experimental and Calculated Structural Amplitudes for the Hydroxide Component of the Structure of Phase 2

hkl	$\lvert\phi_{ex}\rvert$	ϕ_{calc}	*hkl*	$\lvert\phi_{ex}\rvert$	ϕ_{calc}
010	1.72	2.21	130	1.04	0.48
020	6.65	6.6	200	1.63	2.2
030	0.90	0.6	210	1.83	2.90
040	1.56	1.2	220	0.85	1.04
100	3.06	3.5	230	0.96	0.7
110	1.57	1.21	300	0.95	0.08
120	1.55	1.47	310	1.23	2.3
			B = 2		R = 25, 2%

In the minerals of the tochilinite group, where the sulfide component contains sulfur atoms arranged according to a quasi-quadrate motif, a mutual accommodation of the sulfide and brucite networks takes place. As a result, the structures of tochilinite-I and tochilinite-II are described in terms of a single unit cell. Analyzing the unit cells typical of mackinawite and brucite, the components of tochilinite, one sees that the square network in mackinawite is somewhat stretched along the *a* axis of tochilinite-I, while brucite as a rule contracts along the same direction.

The tendency of the vacancies to be arranged according to the square sulfide motif, as in tochilinite-II (Fig. 5), changes neither the relative orientation of the sulfide and brucite components as compared with tochilinite-I nor their mutual "adjustment."

In Phase 1, where the vacancies have a more simple arrangement (Fig. 13), the brucite com-

TABLE 4. The *x* and *y* Coordinates of Atoms in the Hydroxide Component of the Structure of Phase 2*

	Fe	OH	$H_2O(1)$	$\frac{1}{2}H_2O(2)$
x	0	0.17	0.5	0.5
y	0	0.5	0	0.5

* Coordinates are given for the choice of the unit cell differing from that of Figure 17. In this case a = 4.09 Å, b = 3.68 Å, and the origin of coordinates coincides with the Fe atom.

TABLE 5. Hybrid Structures with a Sulfide Component

Name of mineral	Formula	Sulfide component		Hydroxide component	
	Valleriites				
Valleriite from Loolecop (Africa) (Evans and Allmann, 1968)	$Fe_{1.07}Cu_{0.93}S_2 \cdot 1.526\ [Mg_{0.68}Al_{0.32}(OH)_2]$	$R\bar{3}m$	a = 3.79Å c = 34.10Å	$P\bar{3}m$	a = 3.07Å c = 11.37Å
Valleriite from Kaveltorpe (Sweden) (Organova *et al*, 1973)	$Cu_{0.81}Fe_{1.19}S_2 \cdot 1.51\ [Mg_{0.83}Fe_{0.17}(OH)_2]$	$P\bar{3}m$	a = 3.79Å c = 11.37Å	$P\bar{3}m$	a = 3.08Å c = 11.37Å
	Tochilinite-like minerals				
Tochilinite I (Organova *et al*, 1972)	$6Fe_{0.9}S \cdot 5[Mg_{0.7}Fe_{0.3}(OH)_2]$	$C1$	a = 5.37Å b = 15.60Å c = 10.72Å $\alpha = \gamma = 90°$ $\beta = 95°$		
Tochilinite II (Organova *et al*, 1973a)	$6Fe_{0.8}S \cdot 5[Mg_{0.7}Fe_{0.3}(OH)_2]$	$P1$	a = 8.34Å b = 8.54Å c = 10.74Å α = 87.3° β = 94.5° γ = 92°	$C1$	a = 5.42Å b = 15.65Å c = 10.74Å $\alpha = \gamma = 90°$ β = 95°
	Common unit cell	$P1$	a = 50.04Å b = 51.24Å c = 10.94Å α = 87.3° β = 94.5° γ = 92°		
Phase 1	$2Fe_{0.78}S \cdot 1.57[(Mg,Fe)(OH)_2]$	$P1$	$a = b$ = 3.68Å c = 10.92Å $\alpha = \beta$ = 93.5° γ = 90°	$P1$	a = 8.31Å b = 14.4Å c = 21.84Å $\alpha = \beta$ = 93.5° γ = 90°
Phase 2	$20Fe_{0.78}S \cdot 9[Fe(OH)_23/2H_2O]$		$a = b$ = 3.68Å c = 10.92Å $\alpha = \beta$ = 93.5° γ = 90°		a = 8.18Å b = 3.68Å γ = 90°

ponent has been distributed by a more complicated two-layer regularity.

Finally, it is worthy of note that there occurs a Phase 2 in which, alongside the above-described "chessboard" sulfide layers, there are layers with a structure differing from that of brucite.

The difference between the valleriite and mackinawite-like sulfide layers occurring in the tochilinite group concerns not merely structure, but also composition. All known valleriites contain copper. It never occurs in tochilinites, but the sulfide layer of tochilinite always contains vacancies.

Using the selected area patterns, one can readily distinguish between valleriite-like and tochilinite-like structures and identify the distribution law of vacancies in the sulfide layers.

References

BERNER, R. A. (1962) Tetragonal iron sulfide. *Science*, **137**, 669.

CLARK, A. H. (1970) A probable second occurrence of Jambor's "fibrous iron sulfide." *Am. Mineral.* **55**, 283–285.

EVANS, H. T., AND R. ALLMAN, JR. (1968) The crystal structure and crystal chemistry of valleriite. *Z. Kristallogr.* **127**, 73–93.

HARRIS, D. C., AND D. J. VAUGHAN (1972) Two fibrous iron sulfides and valleriite from Cyprus with new data on valleriite. *Am. Mineral.* **57**, 1037–1053.

JAMBOR, I. L. (1969) Coalingite from the Muskox Intrusion. *Am. Mineral.* **54**, 437–448.

ORGANOVA, N. I., A. D. GENKIN, V. A. DRITS, A. L. DMITRIK, AND O. V. KUZMINA (1971). Tochilinit—novyi—sulfid-gidrookisel zheleza i magniya (Tochilinite: a new sulfide hydroxide of iron and magnesium). *Zap. Mineral. obschestva*, **4**, 477–487.

———, V. A. DRITS, AND A. L. DMITRIK (1972) Structurnoe issledovanie tochilinita: I. izometricheskaya raznovidnost. (Structural study of tochilinite: I. Granular modification). *Kristallografiya*, **4**, 761–767.

———, ———, AND ——— (1973a) Structurnoe issledovanie tochilinita: II. igol'chataya raznovidnosti: III. neobychnye difraczionnye kartiny. (Structural study of tochilinite: II. acicular modification, III. unusual diffraction patterns). *Kristallografiya*, **5**, 960–965.

———, ———, AND ——— (1973b) Ob odnosloynom valleriite (On one-layer valleriite). *Dokl. Akad. Nauk SSSR*, **212**, 192–195.

VAINSHTEIN, B. K. (1964) *Structure Analyses by Electron Diffraction.* Pergamon Press, Oxford.

ZVYAGIN, B. B. (1967) *Electron Diffraction Analyses of Clay Mineral Structures.* Plenum Press, New York, pp. 95–105.

Manuscript received, December 26, 1972; accepted for publication, August 29, 1973.